Processing and Application of Ceramics 9 [3] (2015) 157–168
DOI: 10.2298/PAC1503157S

Nanomaterials - What energy landscapes can tell us☆

Johann Christian Schön*

Max-Planck-Institute for Solid State Research, Heisenbergstr. 1, D-70569 Stuttgart, Germany

Received 12 June 2015; Received in revised form 24 September 2015; Accepted 27 September 2015

Abstract

Nanomaterials bridge the gaps between crystalline materials, thin films, and molecules, and are of great importance in the design of new classes of materials, since the existence of many modifications of a nano-object for the same overall composition allows us to tune the properties of the nanomaterial. However, the structural analysis of nano-size systems is often difficult and their structural stability is frequently relatively low. Thus, a study of their energy landscape is needed to determine or predict possible structures, and analyse their stability, via the determination of the minima on the landscape and the generalized barriers separating them. In this contribution, we introduce the major concepts of energy landscapes for chemical systems, and present summaries of four applications to nano-materials: a MgO monolayer on a sapphire substrate, possible quasi-two-dimensional carbon-silicon networks, the ab initio energy landscape of Cu_4Ag_4-clusters, and the possible arrangements of ethane molecules on an ideally smooth substrate.

Keywords: *energy landscapes, MgO, graphene/silicene, nanostructures, intermetallic clusters, thin films*

I. Introduction

The development of new devices and their continuous improvement greatly relies on the availability of new materials [1–6]. While there is still much to be gained from the identification and synthesis of new bulk materials, the purposeful design of new materials on the mesoscopic and nanoscopic level offers great new opportunities. For one, materials already well-known in bulk form can exhibit new or modified properties when prepared at nanoscopic sizes. In particular, one might be able to achieve combinations of properties impossible in the bulk. Next, by combining different nanoscopic materials at the nanoscopic or mesoscopic level, completely new materials can be built in a building block-like fashion, that might not be accessible using standard synthesis techniques.

Another fascinating aspect of nanomaterials is that many more polymorphs or conformations can be accessible in a given chemical system. Of course, a macroscopic sample consisting of orders of magnitude more atoms than a nanoscopic object, must exhibit many more, in principle, feasible atom arrangements, by definition. However, at current levels of synthesis technology, this enormous variety of structures is not accessible in a controlled fashion: achieving such a control might actually become reality once we have established a deeper understanding of the possible nanosize compounds in a given chemical system.

In this context, the term "nanomaterial" tends to be interpreted quite liberally. It includes the classic examples of individual molecules and atomic clusters, but also thin films, heterogeneous layered materials consisting of layers with different compositions that are only a few atom layers thick, nano-porous materials, intercalation compounds with different layers of intercalants, mixed cluster compounds, and many more variations. Common to all these nanomaterials is the fact that during the synthesis process, some control must be exerted to generate compositional or structural variation on the nanolevel, or to produce nanosize polymorphs of materials usually synthesized on the bulk level only.

From a theoretical point of view, the challenge posed by the development and understanding of nanomaterials is threefold: Identification of nanosize materials that are stable enough to be of use in scientific or technological applications, study of their properties in general, and their dynamics in particular, and finally the design of routes to their synthesis.

In all three areas, a detailed investigation of the en-

☆Paper presented at *3rd Conference of The Serbian Society for Ceramic Materials, 3CSCS-2015*, Belgrade, Serbia, 2015

* Corresponding author: tel: +49 711 689 1464,
fax: +49 711 689 1662, e-mail: *C.Schoen@fkf.mpg.de*

ergy landscape can be of great help. This is perhaps most obvious in the identification of stable nano-size compounds, which correspond to locally ergodic regions on the landscape. Similarly, the structural dynamics on the atomic level of nanosize compounds, such as molecules or clusters, takes place on the energy landscape of the system, where it moves among the locally ergodic regions. While in bulk materials the details of the transition are often of secondary importance (and are only discussed in terms of large scale changes), the possible atomically resolved landscape trajectories are much more relevant for nano-size objects. The same holds true with respect to the design of optimal synthesis routes, be they of the bottom-up or the top-down variety, or some combination thereof. Here, too, knowledge of intermediary structures, their stability and the possible transitions to neighbouring polymorphs, should allow us to select and adjust the best set of synthesis routes and parameters.

In this paper, we will first introduce some central energy landscape concepts, followed by a short overview of frequently used powerful global and local landscape exploration methods; in the appendix, we present a brief introduction to the modular G42+ code, which allows the application of several of these methods to various types of nanomaterials and their combinations. The second part of the paper will be devoted to the presentation of a number of applications of these energy landscape techniques in the field of nanomaterials.

II. Energy landscape concepts

In general, an energy landscape consists of three elements: a set of configurations or states $\{\vec{x}\}$, a function which assigns to each state $\vec{x}$ a real number $E(\vec{x})$, and a neighbourhood relation, which tells us which states are the neighbours $\{N(\vec{x})\}$ of a given state $\vec{x}$.

The set of configurations can e.g. be a finite set of discrete states, a compact (finite) subset of a continuous space, an infinite set of countably infinitely many discrete states, or an infinite space. Examples of the first kind are e.g. the discrete configurations of a set of localized spin-1/2 atoms aligned to a magnetic axis: for example, a system of N spin-1/2 atoms has 2^N configurations. An example of type two, a finite subset of a continuous space, would be the possible orientations of a molecule in space given by the angles θ ($0 \leq \theta \leq \pi$) and ϕ ($0 \leq \phi \leq 2\pi$). A set of configurations of the third type is e.g. a crystal (in the thermodynamic limit) of complex anions that can only take on a small number of different orientations with respect to the crystal axes at low temperatures. Finally, there are the infinitely many possible arrangements of the N atoms in any chemical system located somewhere in our three-dimensional Euclidean space $\boldsymbol{R}^3$, $\vec{x} = (\vec{x}_1, \ldots, \vec{x}_N)$, or the combination of atom arrangements with the momenta of the atoms, $(\vec{x}, \vec{p})$, where $\vec{p} = (\vec{p}_1, \ldots, \vec{p}_N)$. The $6N$-dimensional space of the $(\vec{x}, \vec{p})$ is the so-called phase space of the system, while the $3N$-dimensional space of the vectors $\vec{x}$ is called the configuration space. In the following, we will focus only on chemical systems.

In general, the energy $E(\vec{x})$ consists of both potential and kinetic energy, $E = E_{pot}(\vec{x}) + E_{kin}(\vec{p})$, but in many cases we are only interested in the potential energy $E_{pot}(\vec{x})$. For non-zero pressures, this is extended to what might be called the "potential enthalpy", $H_{pot}(\vec{x}) = E_{pot}(\vec{x}) + pV(\vec{x})$. For certain specific questions, we sometimes want to study only small parts of the configuration space. To achieve this, we can explicitly restrict the configuration space, of course. However, this can be rather complicated, and thus one employs an alternative: one adds to the standard energy function a so-called penalty function, which assigns very high energy values to those configurations, which we want to avoid, and is zero otherwise. The sum of the energy plus the penalty term is called a cost function, and one often speaks in this case of a cost function landscape instead of an energy landscape. An example of a cost function is the linear combination of the potential energy with the difference between measured and computed X-ray diffractograms, commonly used for X-ray structure solution [7–9].

Finally, there is the neighbourhood relation. There are two types of neighbourhoods, those which reflect the physics of the system, at least of chemical or physical systems, and those which represent the way we want to explore the configuration space. Most intuitive is the neighbourhood in systems with continuous phase or state spaces where we want to study the dynamics according to physical laws such as the Newtonian dynamics. In that case, the neighbourhood is the same as the intuitive neighbourhoods in Euclidean spaces, i.e. the neighbours of a state $\vec{x}$ are those states $\vec{x}'$ that differ by an infinitesimal displacement $\mathrm{d}\vec{x}$ from $\vec{x}$, $\vec{x}' = \vec{x} + \mathrm{d}\vec{x}$. However, already for discrete sets of states, it is obvious that we have much freedom in choosing such a neighbourhood. But besides the study of the physical dynamics of a system, we might want to explore the low-energy states of the system most efficiently, and thus we might define or construct neighbourhoods, which allow us to achieve this goal. In particular when developing so-called global optimization algorithms for finding the minima or maxima of a cost function, much of the secret to success is in the choice of the neighbourhood relation, usually called the moveclass in this context.

The real time evolution of any physical or chemical system corresponds to a trajectory in the configuration or phase space, which can be visualized as the path of a walker on the energy landscape of the system. On the smallest time scales that are typically simulated (femto seconds), the rules according to which the system evolves are Newton's equations, whose solutions lead to the molecular dynamics simulations [10]. But on slightly larger time scales, e.g. those that are longer than typical vibration times, the Newtonian dynamics can be replaced by an appropriate stochastic dynamics [11], in particular when we are studying the evolution of the sys-

tem at constant temperature which requires stochastic-like terms already in the molecular dynamics simulations. This so-called random-walker picture of the time evolution is often implemented via the so-called Monte Carlo algorithm with the Metropolis acceptance criterion [11]: we select a neighbour state $\vec{x}$ in $N(\vec{x})$, compute the energy difference between the two states, $\Delta E = E(\vec{x}') - E(\vec{x})$, and compare the "Boltzmann-like" factor $f = \exp(-\Delta E/k_B T)$ with a random number r drawn from the interval $[0, 1]$. If $f \geq r$, we accept the move, and if $f < r$, we reject it. It can be shown that for reasonable moveclasses $N(\vec{x})$, this procedure leads to a random walk, which visits all states in configuration space according to the Boltzmann probability. Thus after infinite time, the time averages over this trajectory equal the ensemble averages over the configuration space. This equality of time and ensemble average is known as the ergodicity of the system.

The issue of ergodicity is a very important point, which highlights the difference between the kind of complex energy landscape exhibited by chemical systems, and the simple landscape of e.g. a harmonic oscillator. In the case of the harmonic oscillator, the energy landscape has a very low-dimensional configuration space, and furthermore, only one local minimum, which is at the same time the global minimum, and finally, the landscape does not exhibit any labyrinthine features. Thus, there exists only one time scale of interest for the dynamics: the equilibration time t_{eq} of the oscillator, such that for observation times $t_{obs} > t_{eq}$, all time averages equal the ensemble averages of observables O within a predefined accuracy α, $|\langle O\rangle_{ens} - \langle O\rangle_{tobs}| < \alpha$. Thus, the system is globally, and at the same time also locally ergodic [12]. Of course, if we let α become infinitesimally small, then t_{eq} increases to infinity, but for practical purposes, there is a limit to the experimental measurement accuracy, and thus t_{eq} is a finite quantity. Similarly, the observable O, whose averages we compute, also has some influence on the value of the equilibration time, $t_{eq} = t_{eq}(O; \alpha)$.

But for complex energy landscapes, there are many time scales of interest, associated with the so-called locally ergodic regions (LER) of the energy landscape [12–14]. The barrier structure on this landscape is usually so complicated that there exists a multitude of regions of the landscape, where any typical trajectory that starts within such a region R stays within the region for a long enough time such that the time averages along the trajectory are equal to the ensemble averages restricted to this region R, with an accuracy α. The shortest observation time for which this is true is again the equilibration time, but in this case, this is the equilibration time only for the region R, while other regions have different equilibration times. But, it is clear that after a certain time, called the escape time of the region, the random walker on his trajectory will have left the region R with probability β. While this region is still locally equilibrated, the region is no longer locally ergodic: it was only locally ergodic for observation times in the interval $t_{eq}(R; \alpha) < t_{obs} < t_{esc}(R; \beta)$ [12–14]. Nevertheless, on a time scale at which the region is locally ergodic, we are allowed to compute thermodynamic quantities restricted to this region via an ensemble average, i.e. by performing a summation over all the states in the region weighted by the Boltzmann factor. In particular, we can compute the local free energy $F(R) = -k_B T \ln(Z(R))$, with $Z(R) = \sum_{i \in R} \exp(-E_i/k_B T)$.

We note that both equilibration and escape times will depend on the temperature experienced by the system, and therefore the existence and size of locally ergodic regions depend on temperature, too. In general, we can view the energy landscape as function of observation time (see Fig. 1), and we find that for each given value of t_{obs}, the landscape will break up into different locally ergodic regions that can exist on this observation time scale. As t_{obs} grows, many of the former LERs will vanish, often merging in the process into larger regions, but not always: Think of an amorphous compound, where we have local ergodicity on the time scales of vibrational motion. But once we go to longer time scales, the system is only marginally ergodic (indicated by the dashed lines in Fig. 1), i.e. the equilibration time of every region R is never quite reached: $t_{esc}(R) \cong t_{eq}(R)$, which results in so-called aging phenomena [15].

An important point to note is that viewing and constructing the landscape for different observation times does not correspond to watching the time evolution of the system! At each value of t_{obs}, all the LERs are completely independent of each other: they do not know of each other; else they would not be locally ergodic in the first place. It might be more appropriate to treat these t_{obs}-views of the landscape not as snapshots of a process, but as a depiction of all potentially existing metastable regions of the system on this time scale. This subtlety also applies to the interpretation of the often used statement that the system is most likely found in the region with the lowest local free energy, since $p(R) \propto \exp(-F(R)/T)$. However, this statement only makes sense if we deal with a system that has evolved for time scales larger than the global equilibration time t_{eq}^{glo}, i.e. it is already globally ergodic, and we want to make a short measurement on a time scale $t_{obs} \ll t_{eq}^{glo}$. In this case, we will essentially pick a region R at random to study, with probability $p(R)$ from among all regions which are locally ergodic on time scale t_{obs}. For after the total system has equilibrated (having evolved for times larger than t_{eq}^{glo}), we now only know in a probabilistic fashion (according to the Boltzmann probability) the location of the system at the moment when we start our short measurement - all memory of the detailed trajectory the system has followed throughout its time-evolution towards global equilibrium has vanished during the process of global equilibration.

At very low temperatures, the escape times of many local minima of the energy landscape are much larger than the corresponding equilibration times, and thus in-

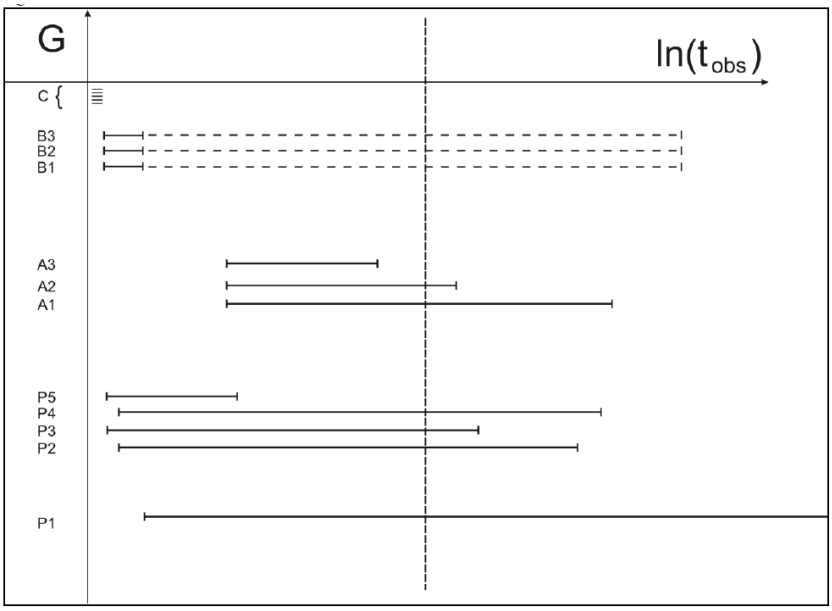

Figure 1. Schematic plot of the range of local ergodicity as function of observation time with free enthalpy *G*, for typical locally ergodic regions of a bulk chemical system for a given temperature: *C* correspond to individual local minima of a particular equilibrium defect configuration of a crystal or amorphous compound; *B1 - B3* are amorphous compounds; *A1 - A3* are solid solutions or structures with rotating complex anions; *P2 - P5* are metastable crystalline compounds; *P1* is the thermodynamically stable state

dividual local minima such as defect configurations of a crystal specified on the atomic level are locally ergodic. And at somewhat elevated temperatures, the LERs often encompass many structurally closely related minima, such as all equilibrium defect configurations associated with a particular crystalline modification, the multiple orientations of complex anions that can convert at high temperatures, or partial occupations of various sites in a crystalline structure. These multi-minima basins also form locally ergodic regions, and represent regions of the energy landscape that correspond to real crystals (i.e., crystals with equilibrium defects), high-temperature crystals with complex anions, or solid solutions, respectively. Thus knowing the LERs as function of observation time and temperature, is essentially equivalent to knowing which compounds can potentially exist in this chemical system and how stable they are.

In particular, information about the local minima on the energy landscape, together with information about the barrier structure and thus the kinetic stability of the local minima and possible transformations among them, serves as an essential first step towards the goal of identifying locally ergodic regions [12–14]. This insight lies behind the wide-spread application of global optimization techniques to the study of complex energy landscapes [13,14,16], where it is of great importance to determine both the global minimum and as many local minima as possible, and the barriers separating them.

But most global optimization methods do not provide us with much information about the barrier structure of the landscape. Thus, it is necessary, to employ additional algorithms that yield the escape times from the locally ergodic regions via the measurement of the generalized barriers separating the LERs. We use the term generalized barriers, since the time evolution of a system with a complex energy landscape is not only controlled by energetic barriers, well-known from simple double-well systems, but also by entropic and dynamical barriers, whose importance increases rapidly with the number of degrees of freedom of the system [17,18]. Thus, the appropriate quantity that describes the dynamics of the system on the time scales beyond the vibrational periods is the so-called probability flow among the locally ergodic regions, e.g. among the minima [19,20]. As mentioned above, we can visualize the time evolution as a stochastic dynamics, and thus we no longer deal with a single trajectory but bundles of trajectories (e.g. by repeating the same stochastic simulation many times with a different random number sequence), and we can register the probability $p(B_i, A)$ to arrive in region B_i after a certain number of steps (or after a certain time) if we have started at region A at time zero. From this flow, we can deduce the transition probabilities among the various minima as function of energy level and temperature, and the probability to remain inside the initial region or return within the measurement time interval, the so-called "return-probability" [19]. These probabilities yield the escape time and thus the degree of kinetic stability of the region. In the final consequence this allows us to model the time evolution of the system as a stochastic process, which can be controlled and optimized, in principle [21].

Finally, we would like to compare the thermodynamic weight of the different locally ergodic regions. The most straightforward approach would be the evalu-

ation of the local free energy via e.g. the vibrational free energy for one or many local minima plus the configurational entropy due to the multitude of local minima inside one LER. More complex methods compute the difference of free energies via umbrella sampling techniques between two or more LERs [22,23]. Finally, we can directly sample the local density of states within the locally ergodic region and perform a Boltzmann summation over all these states to yield the local free energy.

III. Global exploration methods

As indicated above, we need methods that allow us to find local minima, measure barriers and probability flows, and compute the local free energies. The global optimization methods in particular are legion, and we refer to the literature for some (partial) overview over methods that have been employed in the field of chemistry, physics and materials science [13,14,16,24]. We shortly mention the methods that have been employed in the examples described in the next section: simulated annealing [25], basin hopping [26] and genetic algorithms [27]. All three are stochastic exploration techniques; the first two can be performed with many or only one walker at a time, while the third one only makes sense for an ensemble of walkers. The moveclass for generating single walker trajectories in these algorithms for chemical systems consists of displacements of one or several atoms or molecules, rotations and deformations of molecules, changes of the cell parameters of the periodically repeated simulation cell (for crystalline or large amorphous compounds), and exchange of atom positions. The multi-walker moves are typically so-called pair-wise cross-over moves, where the atom positions (and/or cell vectors) belonging to two different configurations (i.e. the walkers) are mixed up and exchanged, in analogy to the exchange of genes in biological systems. While simulated annealing usually employs both small (minor changes in the configuration) and large moves (major changes of the atom arrangement), basin hopping and genetic algorithms predominantly use large moves (hence the term hopping). Here, it has proven useful to follow up each of these large moves with a local minimization, and then to decide the acceptance of the move based on the energy of the minimized configuration.

For the measurement of the probability flow and the estimation of the energy barriers in the examples below, we have employed the threshold algorithm [28,29]. In this method, one starts from a number of local minima determined during a global optimization stage, and performs random walks below a sequence of fixed energy lids or thresholds. During the random walks, one frequently performs a local minimization, in order to determine whether a new minimum has been reached. From the lowest threshold where a new minimum is found, we can estimate the height of the energy barrier between the minima; the probability to find the original minimum yields the so-called return probability and thus the escape time as function of energy; and from the probability to end up in a side minimum, we obtain the transition probability between the minima, again as function of energy lid [19,20,30].

Most of the work presented here has been performed using the so-called G42+ code (see appendix), where many of the algorithms mentioned above have been implemented.

IV. Prototypical example systems

4.1. Magnesium oxide

As a first example, we discuss landscape explorations that have been performed in the system MgO. Besides the bulk modifications, for this system, one is also interested in meso- and nano-size crystallites, and thick and thin films. The interior of the crystallites is expected to consist of some crystalline modification, whose existence and stability can be predicted via the global exploration of the MgO-system using variable simulation cells with periodic boundary conditions. Using simulated annealing and threshold runs [31], we have found, in addition to the ground state NaCl (rock salt)-type polymorph, a large number of metastable modifications exhibiting e.g. the 5-5-structure type [32] (best described as an ionic analogue to the hexagonal modification of boron nitride), the sphalerite-, β-BeO-, and wurtzite-type, plus intergrowth combinations among these (c.f. Fig. 2). Based on the outcome of the threshold runs, all these modifications could be expected to be reasonably stable kinetically.

On the other hand, for nanometer-size clusters, global exploration of such small finite systems by Woodley, Farrow and co-workers [33] has yielded cluster modifications, some of which look like cut-outs from various bulk modifications while others have no corresponding infinite periodic structure. Of particular interest for the work presented here is the fact that among the low-energy stable clusters we encounter cut-outs of the rock salt and of the 5-5-type bulk modifications.

For the present study, we have used the G42+ code to perform additional global explorations of the landscape of possible structures that can form for five different concentrations of Mg- and O-atoms per unit area placed as a monolayer on a specific surface. In the example shown here, we use a ten atom layer thick slab of (001)-Al_2O_3, employing a fixed orthorhombic simulation cell that is periodic in the xy-direction (a = 9.52 Å, b = 8.47 Å, $c = \infty$). The densities varied between ρ = 0.148 and ρ = 0.248 atoms/Å^2 (corresponding density of a monolayer in the experimental bulk NaCl-type structure is about ρ = 0.224 atoms/Å^2). For each concentration of the monolayer, we find that the global minimum corresponds to a cut-out of the MgO bulk ground state (see Figs. 3a,b). However, there exist a multitude of additional atom arrangements, many of which are variations of the NaCl-type structure, of course. But a very interesting class of minimum energy structures that

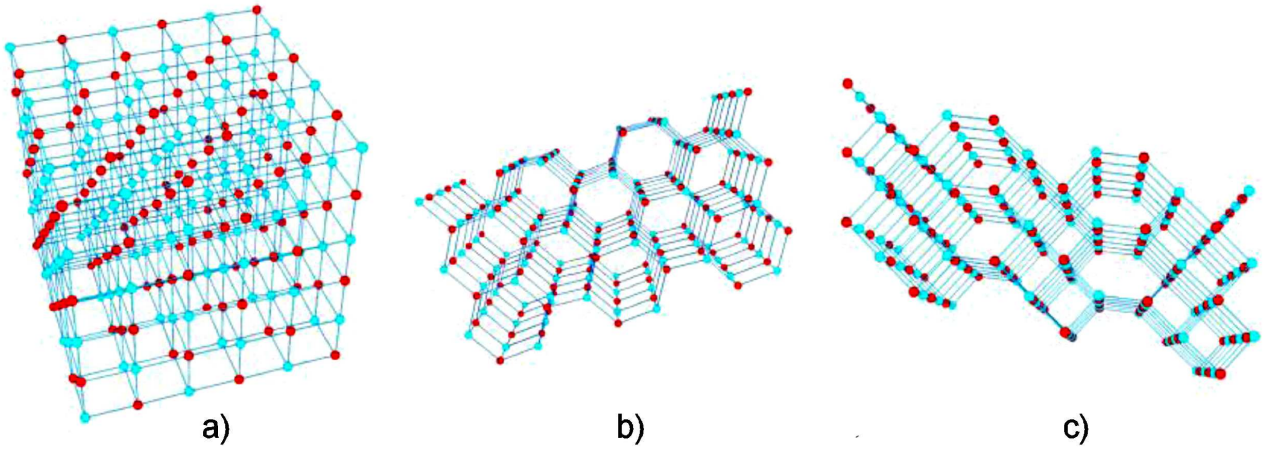

Figure 2. Three examples of modifications of crystalline MgO from global empirical potential searches followed by ab initio minimizations (red = Mg atom, blue = O atom): a) rock salt (NaCl)-type; b) 5-5-type, c) intergrowth of rock salt- and 5-5-type

appear at low densities ($\rho \leq 0.2$ atoms/Å^2) is derived from the 5-5-type structure: for the lowest densities, a complete 5-5-type structure-like layer appears as the structural motif for the whole monolayer, while for the higher densities, we find an intergrowth of the 5-5-type with the NaCl-type MgO-structure (see Figs. 3c,d). In Figs. 3e-h, these monolayer configurations are shown together with the Al_2O_3 substrate. We notice that the substrate leads to distortions in the MgO monolayer which tend to destabilize the NaCl-type layer and promote 5-5-type structure elements. Clearly, the metastable 5-5-type structure has a high likelihood to be accessible synthetically, considering that on all landscapes (bulk, cluster, monolayer) it appears together with the thermodynamically stable bulk structure.

It is very encouraging that recent experimental studies of the epitaxial growth of MgO on sapphire [34] have observed indications of an intermediary structure between the wurtzite and the rocksalt modification (NaCl-type) of MgO with structural properties that are in agreement with the 5-5-type structure. The validity of both theory and experiment is also supported by theoretical studies [35] and experimental thin film work [36] in the analogous ZnO-system, where a similar transition is observed via an intermediary 5-5-type structure.

In all these systems, the global explorations were performed on an empirical potential energy landscape (simulated annealing for crystalline MgO, genetic algorithm for cluster MgO, and simulated annealing + multiple stochastic quenches for the film-like structures, respectively), with refinement of the crystalline and cluster structures on ab initio level. The barrier structure of the crystalline modification was studied using the threshold algorithm on empirical potential level. A natural further step for the study of this system would be the simulation of the actual deposition process of MgO on sapphire, analogously to the one for MgF_2 on sapphire [37], but this is beyond the purview of this presentation that focuses on the insights from energy landscapes.

4.2. Silicon-carbon monolayers

In the past decade, the ability to generate monolayers of carbon experimentally has led to many investigations of the physical and chemical properties of graphene, both in the ideal form and with various kinds of defects [38]. An important analogue is silicene, which is not stable as a free two-dimensional monolayer and requires the presence of a substrate to enforce the perfect two-dimensionality [39].

Thus, it makes sense to ask the question, which alternative periodic carbon networks can exist as two-dimensional monolayers, and whether there exist mixed Si-C-networks that are two-dimensional or whether they tend to buckle if not supported by a substrate. We have employed the G42+ code to address these questions using basin-hopping-simulated annealing for up to eight C/Si-atoms, on an ab initio energy landscape (density functional theory, using Quantum Espresso [40] with pseudo-potentials for Si and C) restricted to stochastic moves only within one monolayer. All the local minima observed were subsequently re-optimized in three dimensions after applying small random displacements, to check their stability as a free-standing monolayer.

Figures 4a-c show the three minimum energy configurations with the lowest energy observed for the composition C:Si = 1:1, all three being derivatives of the graphene structure. We note that when restricted to two dimensions, all the global minima for the compositions C, C_3Si, C_2Si, CSi, CSi_2, CSi_3, and Si are slightly distorted variants of the graphene network, with Si and C freely occupying the locations of the carbon atoms in graphene. These planar minimum energy configurations are stable in three dimensions against small (< 0.5 Å) atom displacements as long as the local concentration of Si-atoms does not become too high; isolated pairs or triplets of Si-atoms appear to be mostly stable, but larger clusters often lead to instabilities. However, it is very noticeable that with increasing Si-content, the number of stable two-dimensional networks in general

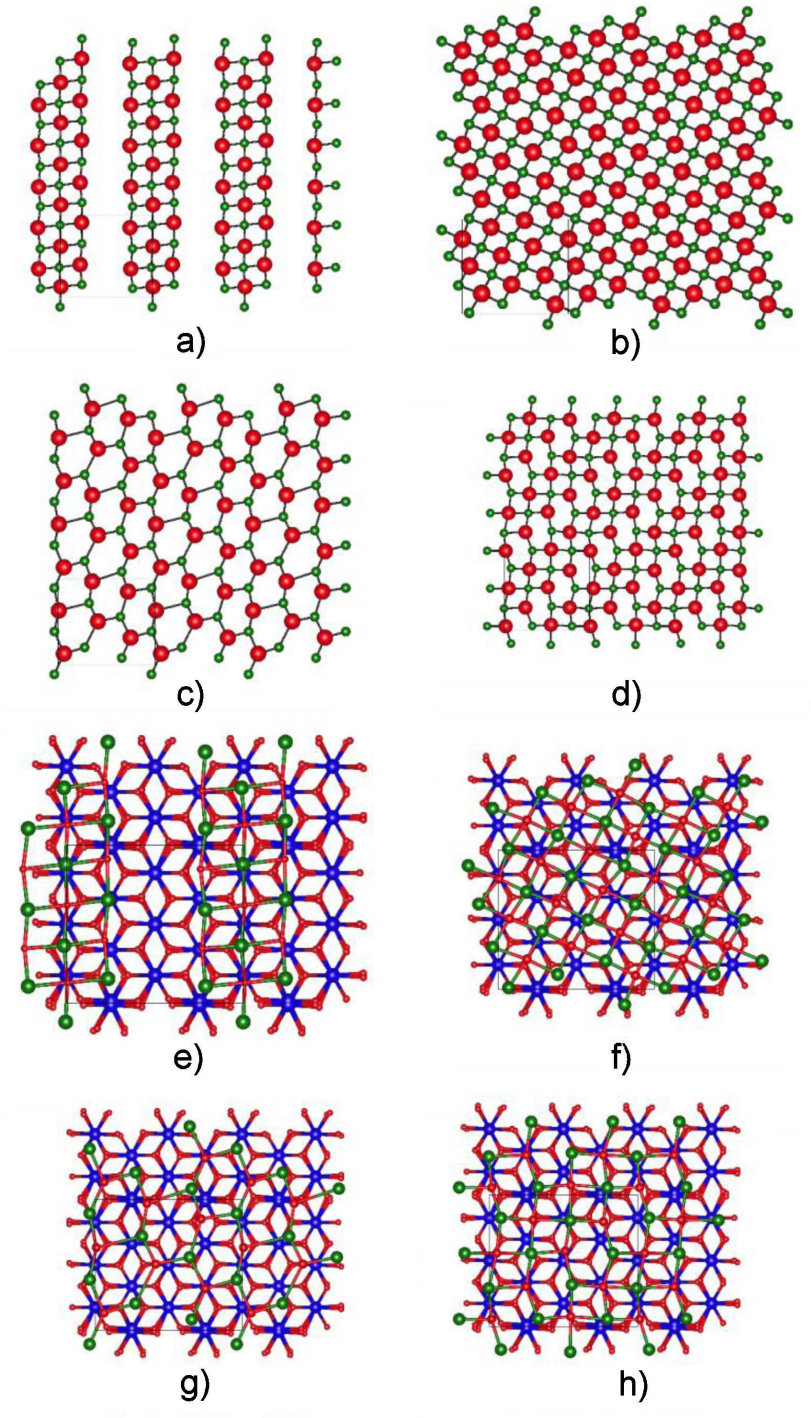

Figure 3. Four instances of local minima of a MgO-monolayer on a sapphire substrate based on global empirical potential (Coulomb+Lennard-Jones interactions) calculations (red = O atom, green = Mg atom, blue = Al atom). In figures a) - d), the substrate is not being shown, while in figures e) - h) the substrate atoms are included: a) and e): global minimum for ρ = 0.148 atoms/Å^2; b) and f): global minimum for ρ = 0.248 atoms/Å^2; c) and g): 5-5-type monolayer for ρ = 0.148 atoms/Å^2; d) and h): intergrowth between rock salt and 5-5-type monolayer for ρ = 0.198 atoms/Å^2. The fixed periodic simulation cell is outlined in black.

decreases, and for Si:C = 3:1 nearly all structures buckle during the 3D-optimization. In this context, we note that the "2D-instability" we discuss here refers to corrugations on the nearest-neighbor level; the long-range instability of every 2D-network cannot be expected to be visible for the small system sizes that can be studied globally on ab initio level.

In addition to the graphene variants, there exist for any composition in the Si/C monolayer system a plethora of alternative structures exhibiting combinations of preferably four-, five-, six-, seven- and eight-rings, which might be accessible to the experiment (see

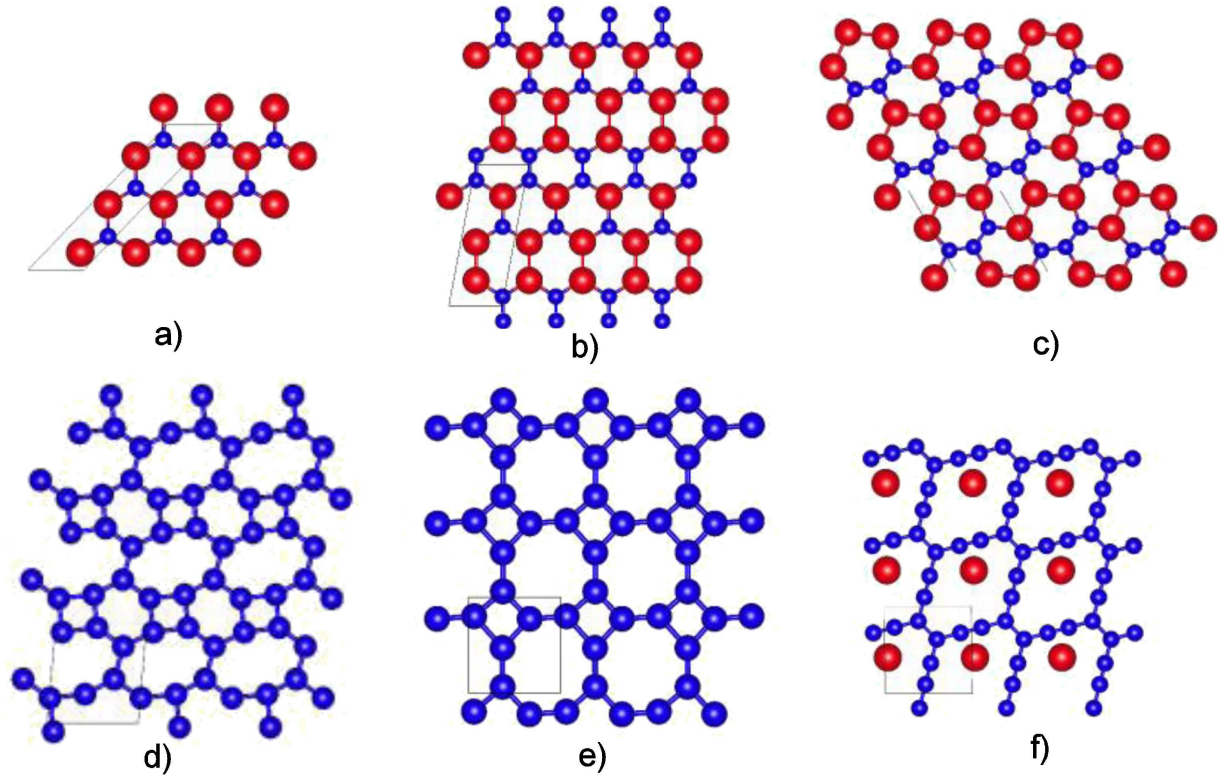

Figure 4. Six examples of local minima for quasi-two-dimensional monolayers in the C/Si-system based on global ab initio energy searches (blue = C atom, red = Si atom): a) - c) three different graphene-derivatives for composition C : Si = 1 : 1 (the global minimum for this composition is the alternating arrangement of Si and C atoms in 4a)); d) (8-6-4)-ring carbon network (also found for several ratios of Si:C); e) (8-4)-ring carbon network (also found for essentially all ratios of Si:C); f) Carbon-network generated around a lattice of exclusion zones depicted as large red discs (analogous to templating of zeolites in three dimensions). The optimized final simulation cell for the structure shown is outlined in black. Note that the shape of the optimized simulation cell is usually different from the conventional unit cell of the modification

Figs. 4d-e). Unsurprisingly the number of non-graphene networks greatly exceeds the graphene-like ones. Configurations with larger rings are also observed, but these are higher in energy and thus are not expected to appear in experiment unless we perform the synthesis on a substrate which exhibits a high density of fixed atom-defects. Figure 4f shows an energetically very favorable carbon network for such a situation, reminiscent of the template effect in zeolite synthesis.

The next step in the investigation might be e.g. the theoretical study of the electronic and thermodynamic properties of these networks as function of composition; however, this goes beyond the remit of this paper which focusses on the information that can be gained from the energy landscape itself.

4.3. Stability of modifications of small clusters

As a third example system, we present a summary of a recent energy landscape study [41] of the intermetallic cluster Cu_4Ag_4. As a first step, a genetic algorithm (implemented in the Birmingham-cluster-genetic-algorithm code [42]) was employed to identify promising configurations on an empirical potential (Gupta-many-body potential) and on an ab initio (DFT, using Quantum Espresso [40]) energy landscape. It was found that the existence and ranking of the various minimum energy structures differed between the empirical and ab initio landscape. We note that this is quite often the case for such small systems - frequently even very good ab initio local minima are not kinetically stable at empirical potential level, and conversely.

Next, the threshold algorithm in the G42+ code was employed on both the Gupta-potential and the ab initio level, yielding tree-graph representations of these landscapes. We find that the various configurations can be allocated to different basins, where some sub-basins of closely related structures are noticeable. Quite generally, the ab initio landscape (see Fig. 5) was more frustrated and exhibited larger energy barriers than the Gupta-potential landscape. In addition, we studied the probability flow (not shown) and the local densities of states, which refined the observations represented in the tree-graphs by depicting the dynamical barriers in the system plus the relative sizes of the various basins. For more details, we refer to reference [41].

4.4. Structure formation of molecules on a surface

Finally, we present the results of the global optimization (using a basin-hopping-simulated annealing algorithm) of a layer of flexible ethane molecules on an ideally smooth substrate with a relatively low fixed density ($\rho \approx 0.025$ ethane molecules/Å^2), employing the

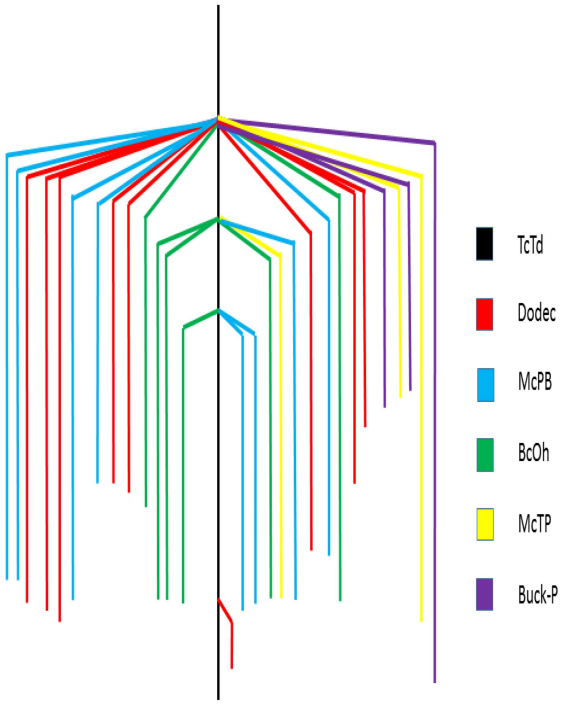

Figure 5. Tree graph of the ab initio energy landscape for Cu_4Ag_4-cluster system based on global threshold explorations. For pictures of the different cluster modifications - labeled TcTd (tetracapped tetrahedron), Dodec (dodecahedron), McPB (monocapped pentagonal bipyramid), BcOh (bicapped octahedron), McTP (monocapped triogonal prism), buck-P (buckled bicapped pentagon), c.f. reference 41.

G42+ code. The energy landscape was explored on the ab initio level (DFT, using Quantum Espresso [40] with pseudo-potentials for C and H), with additional averaged van-der-Waals interactions between the molecule and the substrate. Figure 6 shows three of the many possible quasi-two-dimensional lattices formed by the ethane molecules. We note that the various minimum energy configurations of individual molecules mainly fall into two categories: those, where the axis of the ethane molecule is parallel to the substrate (Fig. 6b), and those, where it is orthogonal (Fig. 6a). Figure 6c shows a typical energy minimum configuration for four molecules / simulation cell.

Again, a very large number of local minima exist on the energy landscape of this system, as it does in all the studies shown in this paper. In this context we note that if we do not force the molecules to remain in a monolayer for most of the global search by allowing arbitrary changes in the shape of the simulation cell, we can end up with multi-layered crystal structures of ethane molecules as the global minimum.

V. Conclusions

In the examples shown in the previous section, we have seen how the study of the energy landscape gives us an overview over the configurations that can potentially exist in a nanomaterial, whether it is a quasi-bulk nano- or meso-crystallite, a nano-meter size cluster, a thin film of a material known already in bulk form, a monolayer of extended (ionic or network- forming) material grown on top of a substrate or free-standing, or the possible arrangements of (organic) molecules on a given substrate surface. In addition, the study of the energy landscape can yield information about the stability of these configurations, and the most likely transformation paths. Finally, by studying the landscapes of the same system on cluster, film, and bulk level, we are able to gain some insights into the routes by which the system evolves, or might evolve, from the atomic to the bulk level.

Acknowledgements: I would like to thank all those who have contributed in various ways to the projects presented here: in particular my collaborators on the

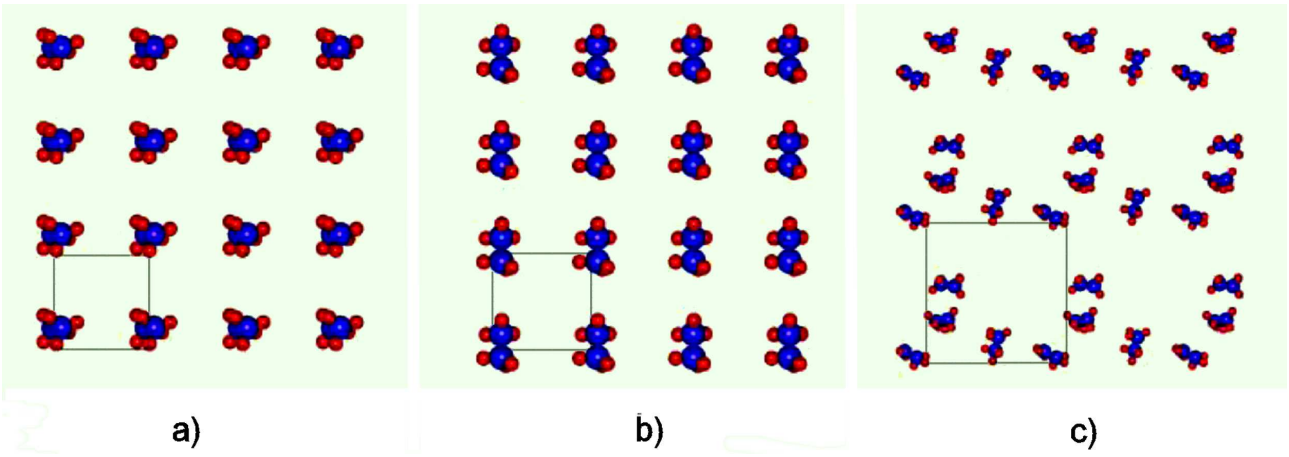

Figure 6. Three possible minimum energy configurations of a monolayer of flexible ethane molecules on a perfectly smooth substrate based on global ab initio energy searches, for fixed density $\rho \approx 0.025$ ethane molecules/Å^2 (blue = carbon atom, red = hydrogen atom): a) ethane molecules standing upright on the surface; b) ethane molecules lying parallel to the surface; c) typical local minimum with several ethane molecules in different orientations and exhibiting different minor distortions. The fixed periodic simulation cell is outlined in black; the smooth idealized substrate surface on which the molecules reside is depicted in light green.

Cu_4Ag_4-study, C. Heard and R.L. Johnston, and furthermore R. Gutzler and D. Fischer for valuable discussions about graphene/silicene networks and MgO-films on substrates, respectively. My special thanks go to C. Heard and S. Neelamraju, who have contributed to the development of the G42+ algorithm, and D. Zagorac for helpful advice in preparing the structure figures.

References

1. R. Ferrando, J. Jellinek, R.L. Johnston, "Nanoalloys: from theory to application of alloy clusters and nanoparticles", *Chem. Rev.*, **108** (2008) 845–910.
2. C.N.R. Rao, A. Müller, A.K. Cheetham (Editors), *The Chemistry of Nanomaterials*, Wiley VCH, Weinheim, 2004.
3. G.A. Ozin, A.C. Arsenault, L. Cademartiri, *Nanochemistry - A Chemical Approach to Nanomaterials*, RSC Publishing, London, 2009.
4. Y. Gogotsi, V. Presser (Editors), *Carbon Nanomaterials*, CRC Press, New York, 2013.
5. H. Hosono, Y. Mishima, H. Takezoe, K.J.D. MacKenzie, *Nanomaterials: From Research to Applications*, Elsevier, Amsterdam, 2006.
6. K.E. Geckeler, H. Nishide (Editors), *Advanced Nanomaterials*, Wiley-VCh, Weinheim, 2009.
7. H. Putz, J.C. Schön, M. Jansen, "Combined method for ab initio structure solution from powder diffraction data", *J. Appl. Cryst.*, **32** (1999) 864–870.
8. O.J. Lanning, S. Habershon, K.D.M. Harris, R.L. Johnston, B.M. Kariuki, E. Tedesco, G.W. Turner, "Definition of a guiding function in global optimization: a hybrid approach combining energy and R-factor in structure solution from powder diffraction data", *Chem. Phys. Lett.*, **317** (2000) 296–303.
9. A.A. Coelho, "Whole-profile structure solution from powder diffraction data using simulated annealing", *J. Appl. Cryst.*, **33** (2000) 899–908.
10. M. Griebel, S. Knapek, G. Zumbusch, *Numerical Simulation in Molecular Dynamics*, Springer, Berlin, 2007.
11. D.P. Landau, K. Binder, *A Guide to Monte Carlo Simulations in Statistical Physics*, Cambridge University Press, Cambridge, 2000.
12. J.C. Schön, "Structure prediction and modelling of solids: An energy landscape point of view", pp. 75–93 in *Proceedings of RIGI-workshop 1998*, ed. J. Schreuer, ETH Zürich, Zürich, 1998.
13. J.C. Schön, M. Jansen, "Determination, prediction, and understanding of structures using the energy landscape approach - Part I and II", *Z. Kristallogr.*, **216** (2001) 307–325 & 361–383.
14. J.C. Schön, M. Jansen, "Prediction, determination and validation of phase diagrams via the global study of energy landscapes", *Int. J. Mater. Res.*, **100** (2009) 135–152.
15. A. Hannemann, J.C. Schön, M. Jansen, P. Sibani, "Non-equilibrium dynamics in amorphous $Si_3B_3N_7$", *J. Phys. Chem. B*, **109** (2005) 11770–11776.
16. A.R. Oganov (Editor), *Modern Methods of Crystal Structure Prediction*, Wiley VCH, Weinheim, 2011.
17. J.C. Schön, M.A. C. Wevers, M. Jansen, "Entropically stabilized region on the energy landscape of an ionic solid", *J. Phys.: Cond. Matter*, **15** (2003) 5479–5486.
18. K.H. Hoffmann, J.C. Schön, "Kinetic features of preferential trapping on energy landcapes", *Found. Phys. Lett.*, **18** (2005) 171–182.
19. M.A.C. Wevers, J.C. Schön, M. Jansen, "Global Aspects of the Energy Landscape of Metastable Crystal Structures in Ionic Compounds", *J. Phys.: Cond. Matter*, **11** (1999) 6487–6499.
20. S. Neelamraju, J.C. Schön, K. Doll, M. Jansen, "Ab initio and empirical energy landscapes of $(MgF_2)_n$ clusters (n = 3,4)", *Phys. Chem. Chem. Phys.*, **14** (2012) 1223–1234.
21. K. H. Hoffmann, J.C. Schön, "Controlled dynamics on energy landscapes", *Eur. Phys. J. B*, **86** (2013) 220.
22. G. Ciccotti, D. Frenkel, I.R. McDonald, *Simulation of Liquids and Solids*, North-Holland, Amsterdam, 1987.
23. D. Chandler, *Introduction to Modern Statistical Mechanics*, Oxford University Press, New York, 1987.
24. S.M. Woodley, C.R.A. Catlow, "Crystal structure prediction from first principles", *Nature Mater.*, **7** (2008) 937–946.
25. S. Kirkpatrick, C.D. Gelatt Jr., M.P. Vecchi, "Optimization by simulated annealing", *Science*, **220** (1983), 671–680.
26. D.J. Wales, J.P.K. Doye, "Global optimization by basin hopping and the Lowest Energy Structures of Lennard-Jones Clusters Containing up to 110 Atoms", *J. Phys. Chem.*, **101** (1997), 5111–5116.
27. J. H. Holland, *Adaptation in Natural and Artificial Systems*, Univ. Mich. Press, Ann Arbor, 1975.
28. J.C. Schön, "Studying the Energy Hypersurface of Multi-Minima Systems - the Threshold and the Lid Algorithm", *Ber. Bunsenges.*, **100** (1996), 1388–1391.
29. J.C. Schön, H. Putz, M. Jansen, "Investigating the energy landscape of continuous systems - the threshold algorithm", *J. Phys.: Cond. Matter*, **8** (1996) 143–156.
30. J.C. Schön, M.A.C. Wevers, M. Jansen, "Characteristic regions on energy landscapes of complex systems", *J. Phys. A: Math. Gen.*, **34** (2001) 4041–4052.
31. J.C. Schön, "Enthalpy landscapes of the earth alkali oxides", *Z. Anorg. Allg. Chem.*, **630** (2004) 2354–2366.
32. J.C. Schön, M. Jansen, "Determination of candidate structures for simple ionic compounds through cell optimisation", *Comp. Mater. Sci.*, **4** (1995) 43–58.
33. M.R. Farrow, Y. Chow, S.M. Woodley, "Structure prediction of nanoclusters; a direct or a pre-screened

search on the energy landscape?", *Phys. Chem. Chem. Phys.*, **16** (2014) 21119–21134.
34. C. Martinez-Boubeta, A.S. Botana, V. Pardo, D. Baldomir, A. Antony, J. Bertomeu, J.M. Rebled, L. Lopez-Conesa, S. Estrade, F. Peiro, "Heteroepitaxial growth of MgO (111) thin films on Al_2O_3 (0001): Evidence of a wurtzite to rocksalt transition", *Phys. Rev. B.*, **86** (2012) 041407(R).
35. D. Zagorac, J.C. Schön, M. Jansen, "Energy landscape investigations using the prescribed path method in the ZnO system", *J. Phys. Chem. C*, **116** (2012) 16726.
36. C. Tusche, H.L. Meyerheim, J. Kirschner, "Observation of depolarized ZnO (0001) monolayers: formation of unreconstructed planar sheets", *Phys. Rev. Lett.*, **99** (2007) 026102.
37. S. Neelamraju, J.C. Schön, M. Jansen, "Atomistic modeling of the low-temperature atom-beam deposition of magnesium fluoride", *Inorg. Chem.*, **54** (2015) 782–791.
38. W. Choi, J.-W. Lee (Editors), *Graphene: Synthesis and Applications*, CRC Press, New York, 2012.
39. A. Kara, H. Enriquez, A.P. Seitsonen, L.C.L.Y. Voon, S. Vizzini, B. Aufray, H. Oughaddou, "A review of silicene - new candidates for electronics", *Surf. Sci. Rep.*, **67** (2012) 1–18.
40. P. Giannozzi, S. Baroni, N. Bonini, M. Calandra, R. Car, C. Cavazzoni, D. Ceresoli, G.L. Chiarotti, M. Cococcioni, I. Dabo, A. Dal Corso, S. Fabris, G. Fratesi, S. de Gironcoli, R. Gebauer, U. Gerstmann, C. Gougoussis, A. Kokalj, M. Lazzeri, L. Martin-Samos, N. Mazari, F. Mauri, R. Mazzarello, S. Paolini, A. Pasquarello, L. Paulatto, C. Sbraccia, S. Scandolo, G. Sclauzero, A.P. Seitsonen, A. Smogunov, P. Umari, R.M. Wentzovitch, "QUANTUM ESPRESSO: a modular and open-source software project for quantum simulations of materials", *J. Phys.: Cond. Matter*, **21** (2009) 395502.
41. C. Heard, J.C. Schön, R.L. Johnston, "Energy landscape exploration of sub-nanometre copper-silver clusters", *Chem. Phys. Chem.*, **16** (2015) 1461–1469.
42. C. Roberts, R.L Johnston, N.T. Wilson, "A genetic algorithm for the structural optimization of Morse clusters", *Theor. Chem. Accounts*, **104** (2000) 123–130.
43. A. Möbius, A. Neklioudov, A. Diaz-Sanchez, K. H. Hoffmann, A. Fachat, M. Schreiber, "Optimization by thermal cycling", *Phys. Rev. Lett.*, **79** (1997) 4297–4301.
44. J.D. Gale, A.L. Rohl, "The general utility lattice program (GULP)", *Mol. Simul.*, **29** (2003) 291–341.
45. H.J.C. Berendsen, D. van der Spoel, R. van Drunen, "GROMACS: A message-passing parallel molecular dynamics implementation", *Comp. Phys. Comm.*, **91** (1995) 43–56.
46. D.A. Pearlman, D.A. Case, J.W. Caldwell, W.S. Ross, T.E. Cheetham III, S. DeBolt, D. Ferguson, G. Seibel, P. Kollman, "AMBER, a package of computer programs for applying molecular mechanics, normal mode analysis, molecular dynamics and free energy calculations to simulate the structural and energetic properties of molecules", *Comp. Phys. Comm.*, **91** (1995) 1–41.
47. V.R. Saunders, R. Dovesi, C. Roetti, R. Orlando, C.M. Zicovich-Wilson, N.M. Harrison, K. Doll, B. Civalleri, I.J. Bush, P. D'Arco, M. Llunell, *CRYSTAL03 User's Manual*; Universita' di Torino, Torino, 2003.
48. K. Koepernik, H. Eschrig, "Full-potential nonorthogonal local-orbital minimum-basis band-structure scheme", *Phys. Rev. B.*, **59** (1999) 1743–1757.
49. J.C. Schön, *G42+ Manual*, Max Planck Institute for Solid State Research, http://www.chemie.uni-bonn.de/ac/schoen/forschung/g42-manual, Stuttgart, 2015.

Appendix: The G42+ code

Many of the explorations presented in section 4 have been performed using the G42+ code. This code has a modular structure, i.e. one can combine a multitude of stochastic landscape exploration algorithms. One can use the code itself to generate a metascript, which allows a nearly unlimited combination of various exploration modules and repetition of this combination with different random numbers / starting structures / parameter choices.

The most important global optimization methods implemented are simulated annealing (with small and large basin-hopping-type moves, plus multi-walker crossover moves) with and without multiple local minimizations in-between, constant temperature Monte-Carlo simulations, parallel tempering with many temperatures and pressures, (multiple) local minimizations such as stochastic quenches and/or gradient descent minimizations, and thermal cycling [43] and multi-quench algorithms. To this are added barrier exploration methods such as the threshold algorithm [28,29], and the prescribed path algorithm [35] (an extension of the nudged elastic band methods to widely separated minima).

As energy functions, both many fast built-in empirical potentials and interfaces to external codes with empirical potential (GULP [44], GROMACS[45], AMBER [46]) and ab initio energy functions (QUANTUM ESPRESSO [40], CRYSTAL [47], FPLO [48]) are available. The systems studied can be periodic in three and two dimensions (with variable simulation cells) or nonperiodic clusters/molecules. Furthermore, we can define arbitrary (periodic or non-periodic) background structures such as substrates or intercalation matrices etc. as the environment whereon or wherein the atoms / molecules of interest move.

The defining elements of each configuration are the three cell vectors, the positions of the atoms and molecules (plus the positions of all the atoms within

each molecule with respect to its center), plus the locations of a number of pseudo-atoms such as vacancies, free electrons, and exclusion zones. Furthermore, we can define perfect substrate surfaces, which interact with the mobile atoms and molecules via average van-der-Waals forces and via image charges if we want to employ conducting substrates. All the cell vectors, and all atom positions regardless of whether the atoms are part of a molecule or independent, and also the positions of the pseudo-atoms can be varied or kept fixed according to the set-up of the problem one wants to study, and what kind of explorations one wishes to perform under which boundary conditions.

For more details, we refer to the G42+ manual [49].